Alejandro O. Sodero[1], Monica Rodriguez-Silva[1], Chiara Salio[3], Marco Sassoè-Pognetto[4] and Jeremy W. Chambers[1,2*] Sab is differentially expressed in the brain and affects neuronal activity.

Bain Research, 1670, 2017, pagg. 76-85.

Sab is differentially expressed in the brain and affects neuronal activity.

Alejandro O. Sodero[1], Monica Rodriguez-Silva[1], Chiara Salio[3], Marco Sassoè-Pognetto[4] and Jeremy W. Chambers[1,2*]

[1]Department of Cellular Biology and Pharmacology, [2]Department of Neuroscience, Herbert Wertheim College of Medicine, Florida International University, Miami, FL 33199.

[3]Department of Veterinary Sciences, [4]Department of Neuroscience, University of Turin, Italy.

*Corresponding Author: Jeremy W. Chambers, Ph.D., Assistant Professor

Herbert Wertheim College of Medicine

Florida International University

AHC4, Room 232

11200 SW 8th Street

Miami, FL 33199

Office: (305) 348-4648

Email: jwchambe @fiu.edu

Running Title: Sab-mediated signaling facilitates neuronal activity

Abstract

Sab is a mitochondrial scaffold protein involved in signaling associated with mitochondrial dysfunction and apoptosis; furthermore, Sab is a crucial signaling platform for neurodegenerative disease. Inhibition of Sab-mediated signaling is effective in models of Parkinson's disease and cerebral ischemia. To determine how this signaling nexus could have a significant effect on disease, we examined the regional abundance of Sab in the brain and sub-neuronal distribution, and we monitored the effect of Sab-mediated signaling on neuronal activity. We found that Sab is widely expressed the adult mouse brain with increased abundance in hippocampus, ventral midbrain, and cerebellum. Sab found in purified synaptosomes and in cultures of primary hippocampal neurons. Microscopy of mouse hippocampal sections confirmed the mitochondrial localization of Sab in the soma, dendrites, and axons. Given the localization and sub-neuronal distribution of Sab, we postulated that Sab-mediated signaling could affect neuronal function, so we measured the impact of inhibiting Sab-mediated events on the spontaneous activity in cultured hippocampal neurons. Treatment with a Sab-inhibitory peptide (Tat-Sab_{KIM1}), but not a scrambled control peptide, decreased the firing frequency and spike amplitudes. Our results demonstrate that brain-specific Sab-mediated signaling plays a role in neuronal activity through the manipulation of mitochondrial physiology by interacting kinases.

Keywords

Hippocampus, Mitogen-activated Protein Kinase, Neuron, Sab, Signal Transduction

1. Introduction

Mitogen-activated protein kinases (MAPKs) are emerging as critical regulators of neurological function and disease. The c-Jun N-terminal kinase (JNK) is a serine/threonine MAPK that is highly expressed and very active in the brain (Brecht et al., 2005; Carboni et al., 1998; Hu et al., 1997; Lee et al., 1999; Lundby et al., 2012) . In fact, JNK isoforms are extensively linked to neuronal development, function, and disease (Coffey, 2014). This diversity of function can be attributed to the fact that there are three (3) JNK isoforms in the brain (JNK1, JNK2, and JNK3), which can be further processed into ten (10) distinct variants (Gupta et al., 1996). The isoforms specifically vary in their tissue and subcellular distributions as well. The JNK1 isoform accounts for most of the JNK activity in the cortex and cerebellum (Tararuk et al., 2006); meanwhile, JNK3 activity dominates the hippocampus and striatum (Brecht et al., 2005). In neurons, JNK1 is found predominantly in the cytosol, while JNK3 is largely nuclear; JNK2, which exhibits the lowest expression in the brain, is distributed between the nucleus and cytosol (Lee et al., 1999). However, subcellular isoform distribution can vary within specific regions of the brain depending on the relative abundance of specific JNK isoform expression in each area.

In the adult brain, JNK signaling affects macromolecular transport and synaptic plasticity. JNK interacts with vesicular structures and binds to microtubule-associated proteins in the brain (Bjorkblom et al., 2005; Cavalli et al., 2005; Coffey et al., 2000; Feltrin et al., 2012; Tararuk et al., 2006). Collectively, these studies indicate that JNK signaling plays a role in vesicle trafficking and deployment during neurotransmission. Furthermore, JNK1-deficient mice have diminished long-term depression, while JNK2-null mice have reduced late phase long-term potentiation (Chen et al., 2005; Li et al., 2007). Additionally, JNK1-deficient mice or mice treated with JNK-selective inhibitors have decreased basal synaptic transmission (Li et al., 2007;

Yang et al., 2011). These studies demonstrate an importance for JNK signaling in neurotransmission.

Efficient neurotransmission in the adult brain requires proper levels of adenosine triphosphate (ATP) and its generation relies on healthy mitochondria. Indeed, perturbations in mitochondrial function are postulated to precede the onset of cognitive decline and neurodegenerative disease (Knott et al., 2008; Lin and Beal, 2006). Consequently, molecular mechanisms regulating mitochondrial physiology have been shown to play crucial roles in neurotransmission as well as neurological disease (Ivannikov et al., 2013; Small et al., 2011). While the impact of nuclear and cytosolic JNK activities are documented in the brain, less is known regarding mitochondrial JNK activity in the brain under physiological conditions (Coffey, 2014). is Sab (SH3 binding protein 5 or SH3BP5) is a scaffold protein present at mitochondria that facilitates MAPK signaling on the organelle (Chambers et al., 2011a; Wiltshire et al., 2004). This subcellular location favors the interaction of Sab with cytoplasmic proteins involved in different signal transduction pathways, facilitating the communication between mitochondria and the rest of the cell. Specifically, the C-terminal portion of Sab contains two kinase interaction motifs (KIMs) possessing consensus binding sites for MAPKs (Wiltshire et al., 2002). Indeed, Sab has interacts with the c-Jun N-terminal kinase (JNK) in response to distinct cellular stimuli, included neurotoxic chemicals (Aoki et al., 2002; Chambers et al., 2013; Win et al., 2011; Win et al., 2014).

There is little information regarding the physiological role of mitochondrial JNK signaling in the adult brain, as most of the studies have focused on the stress responsiveness and disease-specific contexts of mitochondrial JNK. In response to neurological stress, JNK translocates to mitochondria and phosphorylates Bcl-2 family proteins; specifically, Bcl-2 like protein 11 (Bim) and the BH-3 only protein hara-kiri (Hrk) are phosphorylated by JNK during

serum or nerve growth factor withdrawal as well as during ischemia (Harris and Johnson, 2001; Lei and Davis, 2003; Putcha et al., 2001; Putcha et al., 2003). We have demonstrated that mitochondrial JNK signaling can be selectively inhibited by specifically targeting the JNK-Sab interaction. Using a small, cell-permeable peptide (Tat-Sab_{KIM1}) to emulate the JNK binding site on Sab, we blocked mitochondrial JNK signaling and prevented stress-induced apoptosis without disrupting nuclear JNK activity (Chambers et al., 2011a). We used this approach to demonstrate that mitochondrial JNK signaling was a prominent event in the induction of dopaminergic neurodegeneration in adult rats exposed to 6-hydroxydopamine (Chambers et al., 2013). Collectively, these studies demonstrate that mitochondrial JNK signaling occurs in the brain.

Given the contributions of JNK to neurological function, our current study was designed to define the locations of mitochondrial JNK signaling in the adult brain in order to better understand how this signaling nexus contributes to physiological processes in the brain. We examined the abundance of Sab in different regions of the brain, its sub-neuronal localization and a putative role for Sab-mediated signaling in neuronal activity. Sab was found to be constitutively expressed throughout the adult mouse brain. Further, Sab was expressed in primary rat hippocampal cultures, cultured astrocytes, and synaptosomes isolated from adult mice. Sab was found to be largely mitochondrial in axons, dendrites, and soma of hippocampal neurons. Inhibition of Sab-mediated signaling with the Tat-Sab_{KIM1} peptide impaired basal activity as indicated by decreased firing frequency and amplitude of spikes in cultured hippocampal neurons. Taken together, our studies demonstrate that Sab-mediated signaling is involved in normal neurological processes and the physiological role of JNK in the CNS may extend to the regulation mitochondrial biology.

2. Results

2.1 Sab is expressed throughout the adult brain. To determine the potential distribution of mitochondrial JNK (or MAPK) signaling in the brain, we examined the Sab mRNA levels in 49 areas of the adult mouse brain (Figure 1A). Sab expression was widespread in the brain with particularly high levels in the hippocampus (CA1, CA2/CA3 and dentate gyrus), ventral midbrain (*substantia nigra* and ventral tegumental area) and cerebellum (vermis and lobe) (Figure 1A). We next dissected the brains of adult mice, and acquired proteins to examine the relative levels of Sab in distinct areas. Sab was detected in the olfactory bulb, frontal cortex, striatum, hippocampus, ventral midbrain, cerebellum, and brain stem (Figure 1B). In agreement with the RT-PCR data, Sab protein levels were abundant in the hippocampus, ventral midbrain, and cerebellum (Figure 1B). Analysis across six adult mice was conducted and plotted for each region in Figure 1C.

2.2 Sab is expressed in neurons, at synapses, and in astrocytes. Given the brain distribution of Sab and the previously defined roles for JNK in neuronal function, we examined whether Sab was expressed in neurons, specifically at synapses. Cytosolic JNK activity is described as high in the hippocampus; therefore, we cultured hippocampal neurons (with less than 5% of glial cells) and assessed Sab expression by western blot analysis. Sab was found in cultured neurons (Figure 2A). Since JNK has been implicated in synaptic transmission, we purified synaptosomes from adult rat brains. In Figure 2B, four (4) individual synaptosomal preparations show significant levels of Sab. Finally, to evaluate if Sab was expressed in other cells within the brain, we assayed human fetal astrocytes for Sab expression, and as demonstrated in Figure 2C, Sab was expressed in astrocytes.

2.3 Hippocampal Sab is found in axons, dendrites, and synapses. Because cytosolic JNK activity is elevated in the hippocampal neurons and Sab expression is particularly abundant in the

hippocampus, we assessed the subcellular distribution of Sab using immunofluorescence and confocal microscopy in the CA1 hippocampal subfield. Sab presented the prototypic pattern of a mitochondrial protein, characterized by small intracellular puncta that were particularly apparent in the cell body of CA1 neurons and the major dendritic profiles of the *stratum radiatum* (Figure 3A). To confirm the mitochondrial localization of Sab, we performed post-embedding electron microscopy and analyzed the distribution of gold particles in neuronal profiles of the adult mouse hippocampus. As shown in Figure 3, Sab labeling was selectively localized in mitochondria and was generally not associated with other cell organelles. Sab-positive mitochondria were observed in the different sub-neuronal compartments, *i.e.* cell bodies (Figure. 3B), dendrites (Figure 3C) and axon terminals (Figure 3D). Quantification of gold particle density in these compartments revealed a significant enrichment of Sab labeling in mitochondria compared with the surrounding cytoplasm (Table 1). Sab can also be detected in synapses of axonal terminals as illustrated in Figure 3D.

2.4 Inhibition of Sab-mediated signaling impairs spontaneous hippocampal neuron activity. To gain insight into the physiological role of Sab, we measured the spontaneous firing of cultured hippocampal neurons in high potassium using whole-cell patch clamping. Neurons were treated with either PBS, 5μM Tat-Scrambled peptide or 5μM Tat-Sab_{KIM1} (to inhibit Sab-mediated signaling) for 15 minutes prior to recording (Figure 4A). Untreated neurons or neurons treated with the Tat-Scramble peptide had similar spike rates and amplitudes (Figure 4A-C). Cultured hippocampal neurons treated with the Tat-Sab_{KIM1} peptide had a decreased firing frequency and spike amplitude, compared to untreated or scramble peptide-treated neurons (Figure 4B & 4C). These results collectively demonstrate that Sab is strongly expressed in neuronal mitochondria and that Sab-mediated signaling affects neuronal activity.

3. Discussion

MAPKs are crucial components of neurological and cognitive functions, and elevated MAPK signaling is a common feature in neurological disease (Kim and Choi, 2010). Furthermore, mitochondrial MAPK signaling has emerged as a critical regulatory event for cellular and organelle physiology (Horbinski and Chu, 2005). In the current study, we examined the distribution of a MAPK mitochondrial scaffold protein, Sab and its contribution to neuronal function. Sab has been extensively linked to mitochondrial JNK signaling, which has been shown to induce mitochondrial dysfunction and cell death (Chambers et al., 2011a; Chambers and LoGrasso, 2011). Our examination of Sab expression in the brain revealed an enrichment of Sab in the hippocampus, ventral midbrain and cerebellum (Figures 1A & 1B). Notably, Sab expression parallels that of JNK isoforms (JNK1, JNK2, & JNK3), the only known binding partners for Sab in the brain (Carboni et al., 1998). In particular, JNK3, the predominant brain isoform, has its highest activity in the hippocampus of adult mouse brains (Brecht et al., 2005; Carboni et al., 1998; Lein et al., 2007). Given the interaction between JNK and Sab and their high expression, it is feasible to conceive that the JNK-Sab signaling nexus has a basic role in hippocampal physiology.

The regions identified in Figures 1A and 1B support neuronal processes related to learning and memory as well as motor control. Furthermore, Figure 2 demonstrates that Sab is expressed in the synapses of neurons, which reinforces a putative role for this signaling nexus in neurotransmission, especially, when one considers that Sab is found in axon terminals and synapses (Figure 2B and 3D). Additionally, the identification of significant Sab levels in astrocytes may indicate an important role for mitochondrial JNK signaling in other cells within the brain.

Previous research related to Sab employed subcellular fractionation and fluorescent microscopy to determine that Sab is localized to mitochondria (Chambers et al., 2011a; Wiltshire et al., 2002; Win et al., 2011). For the first time, we used electron microscopy to determine the subcellular distribution of Sab. Gold particle labeling of Sab was found to be almost exclusively mitochondrial; intriguingly, Sab was not found to be associated with the ER (Figure 3B). This is interesting as mitochondria are intimately associated with the ER (Nunnari and Suomalainen, 2012). The localization of Sab to mitochondria confirms the potential for this scaffold protein to sequester and concentrate MAPK signaling at mitochondria.

Labeling of Sab was in mitochondria contained in dendritic profiles and axonal terminals (Figures 3B, 3C, and 3D). This is in agreement with the discovery of Sab in synaptosomes (Figures 2A & 2B). The presence of Sab in these subcellular compartments suggests that Sab may play a role in neurotransmission. The distribution of Sab in neurons may polarize the activities of JNK isoforms with similar distributions. JNK3, the prevailing isoform in the hippocampus, appears to be largely relegated to the nucleus; in contrast, JNK1 is found predominantly in the cell body cytoplasm, axons, and dendrites (Coffey et al., 2002; Lee et al., 1999). This similar distribution of Sab and JNK1 may suggest a means by which JNK1 signaling could be enhanced on mitochondria through an interaction with Sab. However, we cannot currently rule out that Sab may interact with other JNK isoforms or MAPKs on neuronal mitochondria.

At present, the precise function of Sab-mediated signaling in neurons is still unclear. One possibility is that Sab on the axonal mitochondria may be required for the expedited transport and recycling of depolarized mitochondria in an energetic demanding area like dendritic profiles and axonal terminals. Mitochondria are essential to synaptic transmission, as these organelle provide ATP and calcium (Ivannikov et al., 2013). MAPKs, specifically JNK, have been shown

to impact mitochondrial dynamics (Leboucher et al., 2012; Pyakurel et al., 2015). JNK has been shown to phosphorylate Mfn2 causing its degradation, which ultimately produced a fragmented mitochondrial network (Leboucher et al., 2012); likewise, ERK has been shown to act in the similar fashion with Mfn1 (Pyakurel et al., 2015). Sab could be the scaffold protein that facilitates these interactions. Thus, the Sab-MAPK interaction could be crucial to releasing mitochondria from the network in the cell body for use in axons and dendrites. One of the roles for JNK in the adult brain is in the transport of macromolecular complexes to and from the synapse via an interaction with molecular motor proteins (Horiuchi et al., 2007; Verhey et al., 2001). One could also surmise that Sab is required to transport mitochondria to the synapse in a JNK-dependent manner. The roles of Sab-mediated signaling in axons and neurotransmission are under active investigation in our lab.

Based on the expression and broad distribution of Sab in the brain and the complementary distribution of cytosolic JNK activity, we reasoned that Sab-mediated signaling may have a role in basic neurophysiology. Herein, we report that inhibition of Sab-mediated signaling by the Tat-Sab_{KIM1} peptide significantly reduces the activity of cultured hippocampal neurons. In our electrophysiology experiments, inhibiting the Sab-JNK interaction caused a rapid reduction in neuronal activity. A similar effect has been noticed with JNK selective inhibitors *in vitro* and *in vivo* (Coffey, 2014; Yang et al., 2011). Wherein, small molecule JNK inhibitors induced a decrease in basal synaptic transmission. We propose that the effects of the Tat-Sab_{KIM1} peptide are compatible with diminished basal activity caused by a loss of mitochondrial JNK activity; however, we cannot preclude that the Tat-Sab_{KIM1} peptide may be acting as a global JNK inhibitor (targeting both nuclear and mitochondrial signaling) in neurons. Alternatively, it is possible that impairing neuronal Sab-mediated signaling could impair mitochondrial function or induce dysfunction that would lead to an inability to support neuronal firing resulting in the

decreased spike rate and amplitude observed in our studies (Figure 4). Nonetheless, we suggest that Sab may be a novel platform for the regulation of synaptic transmission due to Sab's distribution in the brain and neurons and its potential role in spontaneous activity.

In this work, we have found that the mitochondrial MAPK scaffold protein Sab is well distributed throughout the adult brain. Sab is specifically enriched in the hippocampus, ventral midbrain, and cerebellum. Sab expression overlaps with that of JNK isoforms. Sab is present in neurons in the cell body, axons, and dendrites, and it is detected in synaptosomes suggesting that Sab-mediated signaling is present in synapses; furthermore, inhibition of Sab-mediated signaling impaired spontaneous firing of cultured hippocampal neurons. These data reinforce the importance of mitochondrial MAPK signaling in neurological function and disease. These studies represent a new perspective for MAPK signaling in the brain; wherein, regulation of subcellular MAPK signaling could be an essential factor in the balance of healthy cognitive function and neurodegenerative disease.

4. Materials and Methods

4.1 Ethical Standards and Animal Housing/Care: All experiments were approved by the institutional committees for animal care and utilization at Florida International University and the University of Torino; furthermore, studies were performed in accordance with the Society of Neuroscience and Italian guidelines. C57BL/6 mice (Jackson Laboratories, Bar Harbor, ME) were purchased at 4 weeks of age for studies conducted at FIU, while Sprague-Dawley rats (Harlan Laboratories, Indianapolis, IN) were purchased at 8 weeks of age. Mice were housed in sex-matched cages with no more than five (5) mice per cage, while rats were housed in pairs. Animals were allowed to feed ad libitum and were provided standard chow.

4.2 Sample acquisition and brain dissection: Mice and rats were euthanized and the brains were removed as described in our previous work. For RT-PCR analyses, brains from six (6) animals

were sectioned into 0.5mm slices using a mouse brain matrix and frozen. For the microdissection of individual brain regions, specific slices were bilaterally punched with a 0.5mm diameter needle (Kasukawa et al., 2011). Two (2) slices were surveyed per animal for specific brain regions to assure replication within animals. For protein analysis, brains were dissected as previously described to isolate the olfactory bulb, frontal cortex, striatum, hippocampus, ventral midbrain, cerebellum, and brain stem (Spijker, 2011). For a ventral midbrain isolate that was devoid of hippocampus, cortex, cerebellum, and brain stem, we dissected the brain between -6.38 and -2.6 bregma. The brain stem was considered the region between the ventral midbrain and spinal cord minus the cerebellum; this section specifically contained the pons and medulla. The dissected regions of the brains were then homogenized in T-PER (Thermo-Fisher Scientific) supplemented with protease and phosphatase inhibitors. Homogenates were then analyzed by western blot analysis as described below. Human fetal astrocytes were purchased from ScienCell Research Laboratories (Carlsbad California), and cultured according to manufacturer's instructions. Astrocytes were lysed and analyzed by western blot analysis according to our previously published protocol (Chambers et al., 2011e; Chambers et al., 2013).

4.3 RT-PCR detection of Sab: RNA was isolated from tissue punches using the Trizol reagent, and cDNA was synthesized using Superscript II-mediated reverse transcription from 0.4μg of total RNA. RT-PCR was performed in the ABI Prism 7500 instrument with SYBR Green reagents as previously described (Kasukawa et al., 2011). To determine the Sab levels across specific brain regions, we used a probe specific for a 130bp stretch near the 5'-end of the Sab ORF (5'-CGGAGCCGAAATCCTGCCG-3' and 5'-GACTGATTTAATTCTC-3'). RT-PCR results were normalized to both 18S rRNA and GAPDH levels in the brain. Data are presented in $\log_2$ format.

4.4 Primary hippocampal cultures: Mouse hippocampal neurons purchased from Gibco Life Technologies (A15587, Invitrogen, Carlsbad, CA) were plated in plastic 6-well plates, previously coated with 0.1 mg/mL of poly-L-lysine. The plating density was $1.6x10^5$ cells/well. Neurons were grown for fourteen (14) days in Neurobasal medium supplemented with 2% B27 and 0.5 mM L-glutamine, at 37°C and 5% CO_2.

4.5 Purification of synaptosomes: Synaptosomes were purified from Sprague Dawley rat brains (excluding the cerebellum) as previously described elsewhere (Sodero et al, 2012)(Pilo Boyl et al., 2007). Rats were used to provide a larger preparation of synaptosomes in the event mitochondria needed to be purified for western blot analysis. Briefly, the brains were quickly removed, the olfactory bulb and cerebellum were dissected out, and the tissue was homogenized in ice-cold buffer (320 mM sucrose, 1 mM EDTA and 5 mM HEPES; pH 7.4). The homogenization consisted of eight strokes in a glass-Teflon homogenizer. The homogenate was spun at 3,000xg for 10 minutes. Then, the supernatant was spun at 14,000xg for 10 minutes. The pelleted crude synaptosomes were suspended in Kreb's-Ringer buffer (140 mM NaCl, 5 mM KCl, 5 mM glucose, 1 mM EDTA and 10 mM HEPES; pH 7.4) and mixed with Percoll to reach a final Percoll concentration of 45%. The samples were spun at 18,000xg for 2 minutes and the synaptosomes were recovered from the top of the Percoll suspension. Finally, the synaptosomes were washed in Kreb's-Ringer buffer by spinning them at 18000xg for 30 seconds.

4.6 Lysis and Immunoblotting: Cultured neurons were washed 2 times with ice-cold PBS and then harvested in Radioimmunoprecipitation Assay (RIPA) buffer (50mM Tris-HCl, 150mM NaCl, 1% NP-40, 0.5% sodium deoxycholate and 0.1% sodium dodecyl sulfate, 5mM EDTA and 1mM EGTA; pH 7.4) containing HALT® protease inhibitor and phosphatase inhibitor cocktails (Thermo Scientific, Waltham, MA). The lysate was cleared by centrifugation at 12,000 RPM for 10 minutes. Purified synaptosomes and brain regions were also lysed in RIPA buffer. The protein

concentration of the different lysates was assessed in triplicates using the BCA Protein Assay (Pierce Biotechnology, Rockford, IL). Equivalent amounts of total protein were separated by SDS-PAGE and then transferred to nitrocellulose membranes. The membranes were blocked with 3% BSA in TBS containing 0.1% (v/v) Tween-20 at room temperature for 1 hour, and then probed overnight with mouse monoclonal anti-Sab (1/1,000; Novus Biologicals #H00009467-M01) and rabbit monoclonal anti GAPDH (1/1,000; Cell Signaling Technology #5174). The membranes were then incubated with appropriate fluorescent secondary antibodies (1/20,000; DyLight Anti-mouse 800 and Anti-rabbit 680, Cell Signaling Technologies, #5257 and #5366) for 1 hour at room temperature, and finally scanned using a Li-Cor Biosciences Odyssey CLx device. Images were quantified with the Image J 1.48v software (NIH, USA).

4.7 Confocal microscopy: Anesthetized mice were perfused with Ringer's solution followed by 1% formaldehyde in 0.1 M phosphate buffer (PB). The brain was dissected and cut with a vibratome (100 μm). Free-floating hippocampal sections were pre-incubated in 0.02 M PBS containing 5% normal goat serum (PBS–5% NGS) for 30 min, and then incubated overnight in mouse monoclonal anti-Sab diluted 1/500. Sections were then incubated for 1 hour in Alexa Fluor 488 anti-mouse IgG secondary antibodies (1/500), washed in PBS and mounted in Vectashield (Vector Laboratories) (Pilo Boyl et al., 2007). Routine immunocytochemical controls included the omission of the primary antibody. Images were acquired using a Zeiss Pascal confocal laser scanning microscope.

4.8 Post-embedding electron microscopy: Hippocampal sections were obtained from tissue blocks that had been freeze-substituted with methanol and embedded in Lowicryl HM20 for a previous study (Pilo Boyl et al., 2007). Postembedding immunogold labeling was performed on ultrathin sections using goat anti-mouse secondary antibodies coupled to 10 nm colloidal gold particles (British BioCell International, Cardiff, UK). All procedures have been described in

detail in Sassoè-Pognetto and Ottersen (2000). The grids were observed with a JEM-1010 transmission electron microscope (Jeol, Japan) equipped with a side-mounted CCD camera (Mega View III, Olympus Soft Imaging System, Germany). Gold labeling was quantified in randomly selected grid squares in CA1 *stratum pyramidale* (cell bodies) and *stratum radiatum* (dendrites and axon terminals) in sections from three mice (Sassoè-Pognetto and Ottersen, 2000). The area of profiles was measured using the Image J software.

4.9 Electrophysiology: Whole-cell patch clamp recordings were performed on pairs of synaptically-linked cultured hippocampal neurons grown on coverslips for 14 days (Balena et al., 2008; Hamill et al., 1981). The neurons were placed in artificial cerebrospinal fluid (ACSF – 130mM NaCl, 2.5mM KCl, 15mM HEPES, 1.3mM NaH_2PO_4, 10mM glucose, 2mM $CaCl_2$, and 2mM $MgSO_4$, pH 7.4) and adapted for 30 minutes. The cells were then transferred to a recording solution containing 145mM NaCl, 2.5mM KCl, 2mM $CaCl_2$, 1mM $MgCl_2$, and 10mM HEPES, pH 7.4. For high potassium experiments with concentration of KCl was increased to 25mM. The recording pipettes were pulled from glass capillaries with a resistance of 4-10MΩ, and the pipette were filled with a solution of 135mM K-gluconate, 2mM $MgCl_2$, 10mM HEPES, 7mM NaCl, and 2mM Na_2ATP, pH 7.2 with an osmolarity of 270mOsm. Signals were recorded using an AxoPatch 200B amplifier with 2-kHz filter (Molecular Devices). Data were transferred from the pCLAMP 10 software (Molecular Devices) to GraphPad Prism 6.0 for analysis.

To determine the effect of Sab-mediated signaling on spontaneous firing, primary hippocampal neurons adapting in ACSF were treated with either PBS, 5μM Tat-Sab_{KIM1} or the Tat-Scramble control for the final 15 minutes of acclimation. Neurons were then place in the extracellular solution mention above containing the same concentrations of peptide. To induce spontaneous firing, the potassium concentration in the solution was increased to 25mM. Signals were recorded for 30 seconds following the addition of potassium.

4.10 Statistical analysis and replicates: Data were analyzed using one-sided analysis of variance (ANOVA) and Mann-Whitney tests. For all studies a minimum of three biological replicates or three animals were required.

5. Acknowledgements

The authors would like to acknowledge the generous start-up funds provided to J.W.C. by the Herbert Wertheim College of Medicine and Florida International University.

6. Funding

This work has been supported by a generous start-up fund provided by the Herbert Wertheim College of Medicine and Florida International University to JWC. This research did not receive any specific grant from funding agencies in the public, commercial, or not-for-profit sectors.

7. References

Aoki, H., Kang, P.M., Hampe, J., Yoshimura, K., Noma, T., Matsuzaki, M., Izumo, S., 2002. Direct activation of mitochondrial apoptosis machinery by c-Jun N-terminal kinase in adult cardiac myocytes. J Biol Chem. 277**,** 10244-50.

Balena, T., Acton, B.A., Koval, D., Woodin, M.A., 2008. Extracellular potassium regulates the chloride reversal potential in cultured hippocampal neurons. Brain Research. 1205**,** 12-20.

Bjorkblom, B., Ostman, N., Hongisto, V., Komarovski, V., Filen, J.J., Nyman, T.A., Kallunki, T., Courtney, M.J., Coffey, E.T., 2005. Constitutively active cytoplasmic c-Jun N-terminal kinase 1 is a dominant regulator of dendritic architecture: role of microtubule-associated protein 2 as an effector. J Neurosci. 25**,** 6350-61.

Brecht, S., Kirchhof, R., Chromik, A., Willesen, M., Nicolaus, T., Raivich, G., Wessig, J., Waetzig, V., Goetz, M., Claussen, M., Pearse, D., Kuan, C.Y., Vaudano, E., Behrens, A.,

Wagner, E., Flavell, R.A., Davis, R.J., Herdegen, T., 2005. Specific pathophysiological functions of JNK isoforms in the brain. Eur J Neurosci. 21**,** 363-77.

Carboni, L., Carletti, R., Tacconi, S., Corti, C., Ferraguti, F., 1998. Differential expression of SAPK isoforms in the rat brain. An in situ hybridisation study in the adult rat brain and during post-natal development. Brain Res Mol Brain Res. 60**,** 57-68.

Cavalli, V., Kujala, P., Klumperman, J., Goldstein, L.S., 2005. Sunday Driver links axonal transport to damage signaling. J Cell Biol. 168**,** 775-87.

Chambers, J.W., Cherry, L., Laughlin, J.D., Figuera-Losada, M., Lograsso, P.V., 2011a. Selective inhibition of mitochondrial JNK signaling achieved using peptide mimicry of the Sab kinase interacting motif-1 (KIM1). ACS Chem Biol. 6**,** 808-18.

Chambers, J.W., LoGrasso, P.V., 2011. Mitochondrial c-Jun N-terminal kinase (JNK) signaling initiates physiological changes resulting in amplification of reactive oxygen species generation. J Biol Chem. 286**,** 16052-62.

Chambers, J.W., Pachori, A., Howard, S., Ganno, M., Hansen, D., Jr., Kamenecka, T., Song, X., Duckett, D., Chen, W., Ling, Y.Y., Cherry, L., Cameron, M.D., Lin, L., Ruiz, C.H., Lograsso, P., 2011e. Small Molecule c-jun-N-terminal Kinase (JNK) Inhibitors Protect Dopaminergic Neurons in a Model of Parkinson's Disease. ACS Chem Neurosci. 2**,** 198-206.

Chambers, J.W., Howard, S., LoGrasso, P.V., 2013. Blocking c-Jun N-terminal kinase (JNK) translocation to the mitochondria prevents 6-hydroxydopamine-induced toxicity in vitro and in vivo. J Biol Chem. 288**,** 1079-87.

Chen, J.T., Lu, D.H., Chia, C.P., Ruan, D.Y., Sabapathy, K., Xiao, Z.C., 2005. Impaired long-term potentiation in c-Jun N-terminal kinase 2-deficient mice. J Neurochem. 93**,** 463-73.

Coffey, E.T., Hongisto, V., Dickens, M., Davis, R.J., Courtney, M.J., 2000. Dual roles for c-Jun N-terminal kinase in developmental and stress responses in cerebellar granule neurons. J Neurosci. 20**,** 7602-13.

Coffey, E.T., Smiciene, G., Hongisto, V., Cao, J., Brecht, S., Herdegen, T., Courtney, M.J., 2002. c-Jun N-terminal protein kinase (JNK) 2/3 is specifically activated by stress, mediating c-Jun activation, in the presence of constitutive JNK1 activity in cerebellar neurons. J Neurosci. 22**,** 4335-45.

Coffey, E.T., 2014. Nuclear and cytosolic JNK signalling in neurons. Nat Rev Neurosci. 15**,** 285-99.

Feltrin, D., Fusco, L., Witte, H., Moretti, F., Martin, K., Letzelter, M., Fluri, E., Scheiffele, P., Pertz, O., 2012. Growth cone MKK7 mRNA targeting regulates MAP1b-dependent microtubule bundling to control neurite elongation. PLoS Biol. 10**,** e1001439.

Gupta, S., Barrett, T., Whitmarsh, A., Cavanagh, J., Sluss, H., Derijard, B., Davis, R., 1996. Selective interaction of JNK protein kinase isoforms with transcription factors. EMBO J. 15**,** 2760 - 2770.

Hamill, O.P., Marty, A., Neher, E., Sakmann, B., Sigworth, F.J., 1981. Improved patch-clamp techniques for high-resolution current recording from cells and cell-free membrane patches. Pflügers Archiv. 391**,** 85-100.

Harris, C.A., Johnson, E.M., Jr., 2001. BH3-only Bcl-2 family members are coordinately regulated by the JNK pathway and require Bax to induce apoptosis in neurons. J Biol Chem. 276**,** 37754-60.

Horbinski, C., Chu, C.T., 2005. Kinase signaling cascades in the mitochondrion: a matter of life or death. Free Radical Biology and Medicine. 38**,** 2-11.

Horiuchi, D., Collins, C., Bhat, P., Barkus, R., Diantonio, A., Saxton, W., 2007. Control of a kinesin-cargo linkage mechanism by JNK pathway kinases. Curr Biol. 17**,** 1313 - 1317.

Hu, Y., Metzler, B., Xu, Q., 1997. Discordant activation of stress-activated protein kinases or c-Jun NH2-terminal protein kinases in tissues of heat-stressed mice. J Biol Chem. 272**,** 9113-9.

Ivannikov, M., Sugimori, M., Llinás, R., 2013. Synaptic Vesicle Exocytosis in Hippocampal Synaptosomes Correlates Directly with Total Mitochondrial Volume. Journal of Molecular Neuroscience. 49**,** 223-230.

Kasukawa, T., Masumoto, K.H., Nikaido, I., Nagano, M., Uno, K.D., Tsujino, K., Hanashima, C., Shigeyoshi, Y., Ueda, H.R., 2011. Quantitative expression profile of distinct functional regions in the adult mouse brain. PLoS One. 6**,** e23228.

Kim, E.K., Choi, E.-J., 2010. Pathological roles of MAPK signaling pathways in human diseases. Biochimica et Biophysica Acta (BBA) - Molecular Basis of Disease. 1802**,** 396-405.

Knott, A.B., Perkins, G., Schwarzenbacher, R., Bossy-Wetzel, E., 2008. Mitochondrial fragmentation in neurodegeneration. Nat Rev Neurosci. 9**,** 505-18.

Leboucher, Guillaume P., Tsai, Yien C., Yang, M., Shaw, Kristin C., Zhou, M., Veenstra, Timothy D., Glickman, Michael H., Weissman, Allan M., 2012. Stress-Induced Phosphorylation and Proteasomal Degradation of Mitofusin 2 Facilitates Mitochondrial Fragmentation and Apoptosis. Molecular Cell. 47**,** 547-557.

Lee, J.K., Park, J., Lee, Y.D., Lee, S.H., Han, P.L., 1999. Distinct localization of SAPK isoforms in neurons of adult mouse brain implies multiple signaling modes of SAPK pathway. Brain Res Mol Brain Res. 70**,** 116-24.

Lei, K., Davis, R.J., 2003. JNK phosphorylation of Bim-related members of the Bcl2 family induces Bax-dependent apoptosis. Proc Natl Acad Sci U S A. 100**,** 2432-7.

Lein, E.S., Hawrylycz, M.J., Ao, N., Ayres, M., Bensinger, A., Bernard, A., Boe, A.F., Boguski, M.S., Brockway, K.S., Byrnes, E.J., Chen, L., Chen, L., Chen, T.M., Chin, M.C., Chong, J., Crook, B.E., Czaplinska, A., Dang, C.N., Datta, S., Dee, N.R., Desaki, A.L., Desta, T., Diep, E., Dolbeare, T.A., Donelan, M.J., Dong, H.W., Dougherty, J.G., Duncan, B.J., Ebbert, A.J., Eichele, G., Estin, L.K., Faber, C., Facer, B.A., Fields, R., Fischer, S.R., Fliss, T.P., Frensley, C., Gates, S.N., Glattfelder, K.J., Halverson, K.R., Hart, M.R., Hohmann, J.G., Howell, M.P., Jeung, D.P., Johnson, R.A., Karr, P.T., Kawal, R., Kidney, J.M., Knapik, R.H., Kuan, C.L., Lake, J.H., Laramee, A.R., Larsen, K.D., Lau, C., Lemon, T.A., Liang, A.J., Liu, Y., Luong, L.T., Michaels, J., Morgan, J.J., Morgan, R.J., Mortrud, M.T., Mosqueda, N.F., Ng, L.L., Ng, R., Orta, G.J., Overly, C.C., Pak, T.H., Parry, S.E., Pathak, S.D., Pearson, O.C., Puchalski, R.B., Riley, Z.L., Rockett, H.R., Rowland, S.A., Royall, J.J., Ruiz, M.J., Sarno, N.R., Schaffnit, K., Shapovalova, N.V., Sivisay, T., Slaughterbeck, C.R., Smith, S.C., Smith, K.A., Smith, B.I., Sodt, A.J., Stewart, N.N., Stumpf, K.R., Sunkin, S.M., Sutram, M., Tam, A., Teemer, C.D., Thaller, C., Thompson, C.L., Varnam, L.R., Visel, A., Whitlock, R.M., Wohnoutka, P.E., Wolkey, C.K., Wong, V.Y., Wood, M., Yaylaoglu, M.B., Young, R.C., Youngstrom, B.L., Yuan, X.F., Zhang, B., Zwingman, T.A., Jones, A.R., 2007. Genome-wide atlas of gene expression in the adult mouse brain. Nature. 445**,** 168-76.

Li, X.M., Li, C.C., Yu, S.S., Chen, J.T., Sabapathy, K., Ruan, D.Y., 2007. JNK1 contributes to metabotropic glutamate receptor-dependent long-term depression and short-term synaptic plasticity in the mice area hippocampal CA1. Eur J Neurosci. 25**,** 391-6.

Lin, M.T., Beal, M.F., 2006. Mitochondrial dysfunction and oxidative stress in neurodegenerative diseases. Nature. 443**,** 787-95.

Lundby, A., Secher, A., Lage, K., Nordsborg, N.B., Dmytriyev, A., Lundby, C., Olsen, J.V., 2012. Quantitative maps of protein phosphorylation sites across 14 different rat organs and tissues. Nat Commun. 3**,** 876.

Nunnari, J., Suomalainen, A., 2012. Mitochondria: In Sickness and in Health. Cell. 148**,** 1145-1159.

Pilo Boyl, P., Di Nardo, A., Mulle, C., Sassoè-Pognetto, M., Panzanelli, P., Mele, A., Kneussel, M., Costantini, V., Perlas, E., Massimi, M., Vara, H., Giustetto, M., Witke, W., 2007. Profilin2 contributes to synaptic vesicle exocytosis, neuronal excitability, and novelty-seeking behavior. The EMBO Journal. 26**,** 2991-3002.

Putcha, G.V., Moulder, K.L., Golden, J.P., Bouillet, P., Adams, J.A., Strasser, A., Johnson, E.M., 2001. Induction of BIM, a proapoptotic BH3-only BCL-2 family member, is critical for neuronal apoptosis. Neuron. 29**,** 615-28.

Putcha, G.V., Le, S., Frank, S., Besirli, C.G., Clark, K., Chu, B., Alix, S., Youle, R.J., LaMarche, A., Maroney, A.C., Johnson, E.M., Jr., 2003. JNK-mediated BIM phosphorylation potentiates BAX-dependent apoptosis. Neuron. 38**,** 899-914.

Pyakurel, A., Savoia, C., Hess, D., Scorrano, L., 2015. Extracellular Regulated Kinase Phosphorylates Mitofusin 1 to Control Mitochondrial Morphology and Apoptosis. Molecular Cell. 58**,** 244-254.

Sassoè-Pognetto, M., Ottersen, O.P., 2000. Organization of Ionotropic Glutamate Receptors at Dendrodendritic Synapses in the Rat Olfactory Bulb. The Journal of Neuroscience. 20**,** 2192-2201.

Small, S.A., Schobel, S.A., Buxton, R.B., Witter, M.P., Barnes, C.A., 2011. A pathophysiological framework of hippocampal dysfunction in ageing and disease. Nat Rev Neurosci. 12**,** 585-601.

Spijker, S., 2011. Dissection of Rodent Brain Regions. In Neuroproteomics. Vol., W.K. Li, ed.^eds. Humana Press, Totowa, NJ, pp. 13-26.

Tararuk, T., Ostman, N., Li, W., Bjorkblom, B., Padzik, A., Zdrojewska, J., Hongisto, V., Herdegen, T., Konopka, W., Courtney, M.J., Coffey, E.T., 2006. JNK1 phosphorylation of SCG10 determines microtubule dynamics and axodendritic length. J Cell Biol. 173**,** 265-77.

Verhey, K.J., Meyer, D., Deehan, R., Blenis, J., Schnapp, B.J., Rapoport, T.A., Margolis, B., 2001. Cargo of kinesin identified as JIP scaffolding proteins and associated signaling molecules. J Cell Biol. 152**,** 959-70.

Wiltshire, C., Matsushita, M., Tsukada, S., Gillespie, D.A., May, G.H., 2002. A new c-Jun N-terminal kinase (JNK)-interacting protein, Sab (SH3BP5), associates with mitochondria. Biochem J. 367**,** 577-85.

Wiltshire, C., Gillespie, D.A., May, G.H., 2004. Sab (SH3BP5), a novel mitochondria-localized JNK-interacting protein. Biochem Soc Trans. 32**,** 1075-7.

Win, S., Than, T.A., Han, D., Petrovic, L.M., Kaplowitz, N., 2011. c-Jun N-terminal kinase (JNK)-dependent acute liver injury from acetaminophen or tumor necrosis factor (TNF) requires mitochondrial Sab protein expression in mice. J Biol Chem. 286**,** 35071-8.

Win, S., Than, T.A., Fernandez-Checa, J.C., Kaplowitz, N., 2014. JNK interaction with Sab mediates ER stress induced inhibition of mitochondrial respiration and cell death. Cell Death Dis. 5**,** e989.

Yang, H., Courtney, M.J., Martinsson, P., Manahan-Vaughan, D., 2011. Hippocampal long-term depression is enhanced, depotentiation is inhibited and long-term potentiation is unaffected by the application of a selective c-Jun N-terminal kinase inhibitor to freely behaving rats. Eur J Neurosci. 33**,** 1647-55.

8. Figure Legends

Figure 1. Sab is differentially expressed in the adult rodent brain. RT-PCR was conducted to measure the expression levels of Sab in 49 areas of the adult mouse brain. Areas of increased Sab expression are marked as Hippocampus, VTA & SNpc, and Cerebellum (A). A representative western blot analysis of a dissected adult mouse brain showing the expression of Sab in different regions of the mouse brain (B). The relative Sab fluorescence was normalized to actin levels in each region. The average relative Sab expression from six (6) mice is presented for the western images and individual animal expression levels are illustrated as open circles on each column. (C).

Figure 2. Sab is expressed in neurons, at synapses, and in astrocytes. Western blot analysis for Sab expression in primary hippocampal cultures was performed (A). Sab in rat synaptosomes was measured from four (4) adult rats (B). Sab levels were also monitored by western blot in human fetal astrocytes. COX-IV was used as a mitochondrial abundance control and GADPH was used as loading control.

Figure 3. Sab localizes to mitochondria in hippocampal neurons. Sab immunoreactivity is concentrated in mitochondria. A. Confocal image through the hippocampal CA1. Immunolabeling for Sab is characterized by small puncta in the cell body and dendrites of hippocampal neurons. So: *stratum oriens*; Sp: *stratum pyramidale*; Sr: *stratum radiatum*. B. Electron micrograph showing immunogold labeling for Sab in the cell body of a pyramidal neuron. Gold particles decorate mitochondria (Mito),

whereas the nucleus (Nu), Golgi complex (Go) and endoplasmic reticulum (Er) are unlabeled. C. Strong mitochondrial labeling for Sab in a dendritic profile in *stratum radiatum*. D. Axo-spinous synapse in *stratum radiatum*; note the strong immunogold labeling for Sab in two mitochondria within the presynaptic axon terminal (Ax). Sp: dendritic spine. Scale bars: A = 10 mm; B = 250 nm (applies to B-D).

Figure 4. Inhibition of Sab-mediated signaling decreases basal firing frequency and amplitude. Whole-cell patch clamp was performed on cultured hippocampal neurons that had been treated with either PBS (untreated), 5μM Tat-Scramble, or 5μM Tat-Sab_{KIM1} for 15 minutes prior to high potassium treatment and recordings. Representative recordings for each treatment group are shown in (A). The spike frequency (B) and amplitude (C) was determined over 20 seconds for each record for a minimum of four (4) cultures. Each experiment is represented with an open circle on each box and whisker plot (B & C).

1

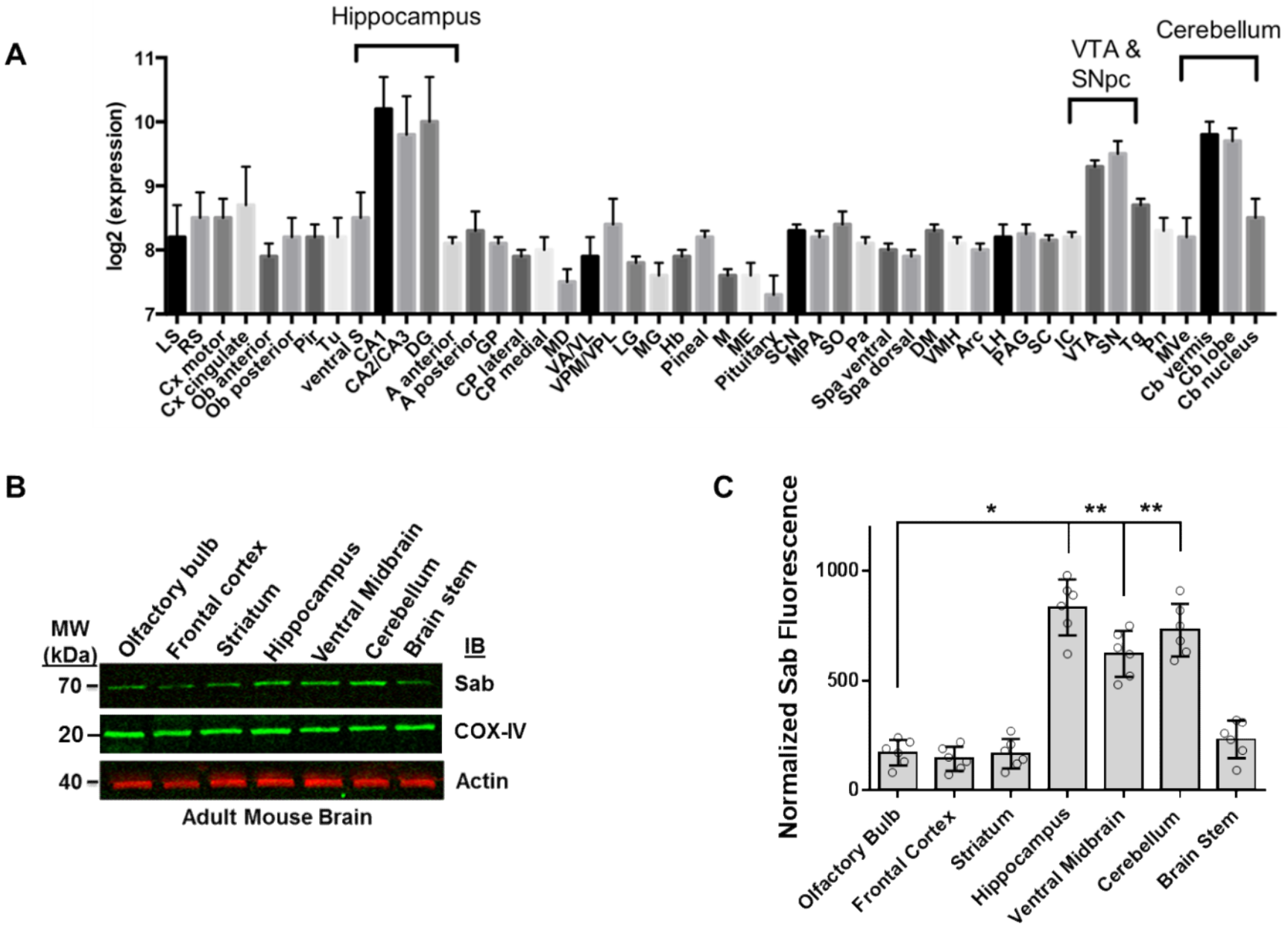
A
Hippocampus
VTA &
SNpc
Cerebellum
log2 (expression)
11
10
9
8
7
LS
RS
Cx motor
Cx cingulate
Ob anterior
Ob posterior
Pir
Tu
ventral S
CA1
CA2/CA3
DG
A anterior
A posterior
GP
CP lateral
CP medial
MD
VA/VL
VPM/VPL
LG
MG
Hb
Pineal
M
ME
Pituitary
SCN
MPA
SO
Pa
Spa ventral
Spa dorsal
DM
VMH
Arc
LH
PAG
SC
IC
VTA
SN
Tg
Pn
MVe
Cb vermis
Cb lobe
Cb nucleus
B
MW
(kDa)
Olfactory bulb
Frontal cortex
Striatum
Hippocampus
Ventral Midbrain
Cerebellum
Brain stem
IB
70
Sab
20
COX-IV
40
Actin
Adult Mouse Brain
C
Normalized Sab Fluorescence
*
**
**
1000
500
0
Olfactory Bulb
Frontal Cortex
Striatum
Hippocampus
Ventral Midbrain
Cerebellum
Brain Stem

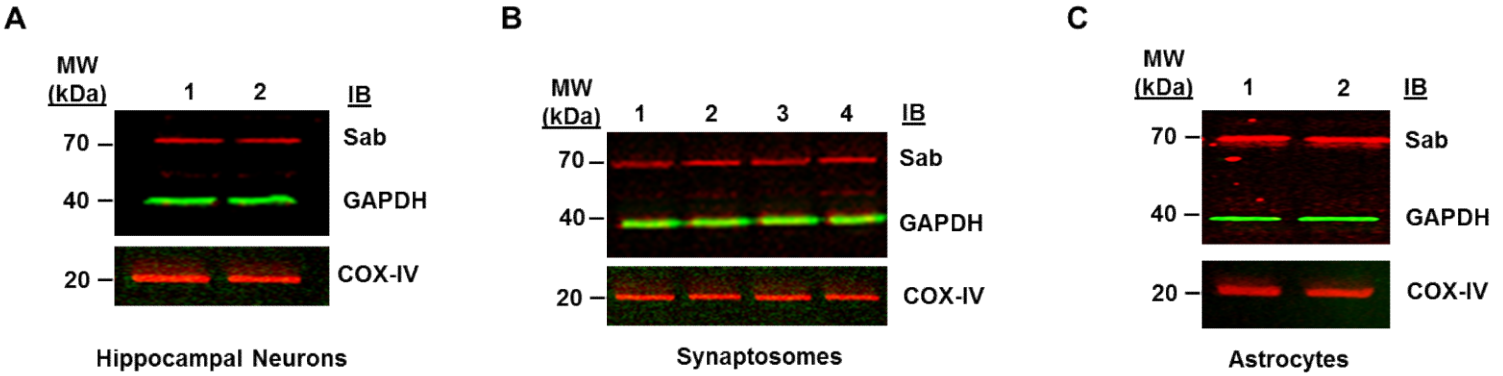
A
MW (kDa)
1
2
IB
70
Sab
40
GAPDH
20
COX-IV
Hippocampal Neurons
B
MW (kDa)
1
2
3
4
IB
70
Sab
40
GAPDH
20
COX-IV
Synaptosomes
C
MW (kDa)
1
2
IB
70
Sab
40
GAPDH
20
COX-IV
Astrocytes

1

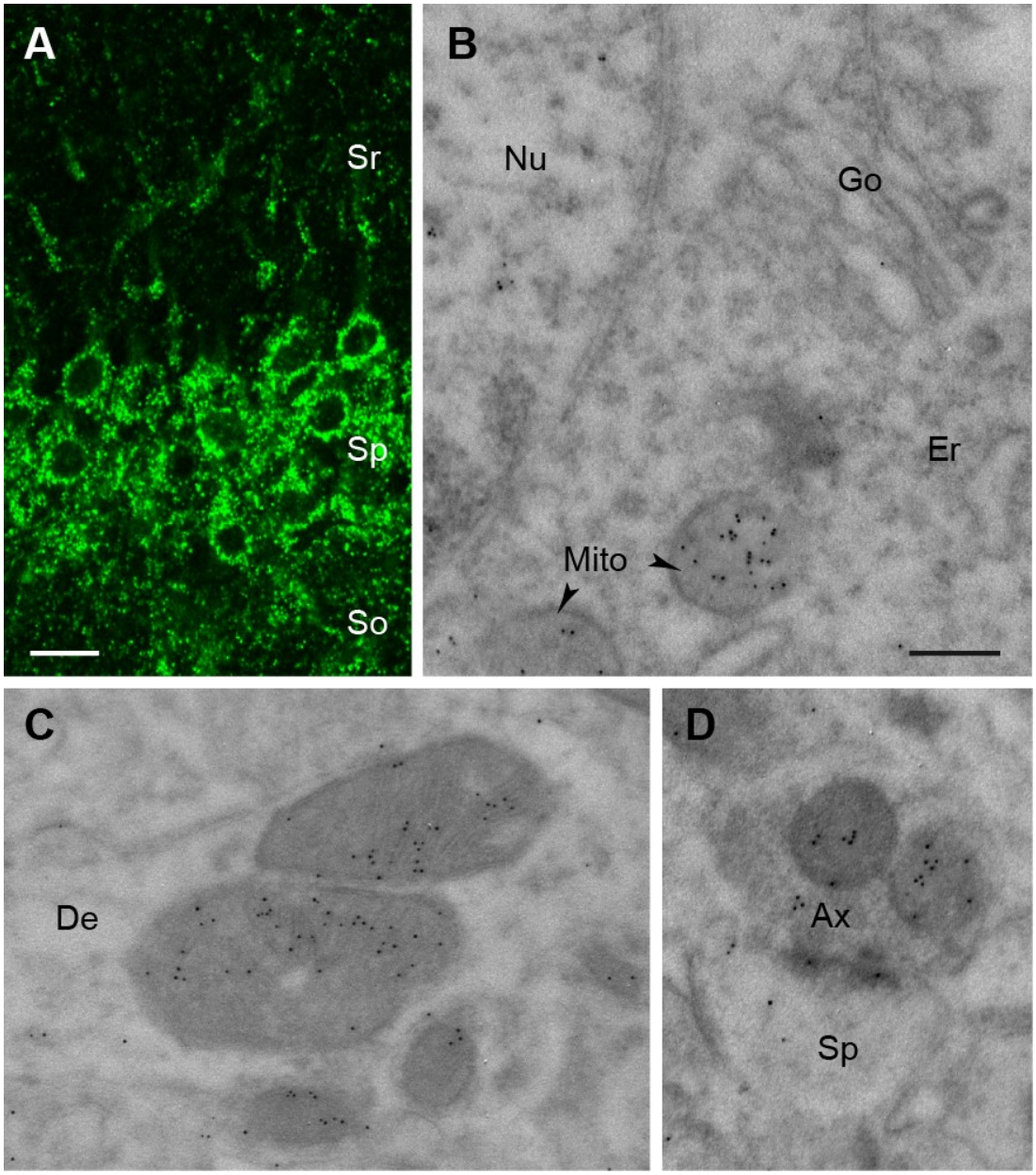

2

3

1

***Table 1:* Gold Particles per Area of Mitochondria and Cytoplasm in Cellular Compartments of Hippocampal Neurons**

	Animal 1	Animal 2	Animal 3
Axon			
Mitochondria	93.56 ± 11.01	88.18 ± 7.24	85.88 ± 8.37
Cytoplasm	32.36 ± 4.60	28.27 ± 2.71	29.02 ± 1.95
Dendrite			
Mitochondria	71.52 ± 6.69	69.42 ± 6.36	65.99 ± 5.03
Cytoplasm	11.19 ± 1.05	10.40 ± 7.08	7.24 ± 0.42
Cell Body			
Mitochondria	62.33 ± 4.64	71.41 ± 4.41	63.83 ± 4.22
Cytoplasm	9.58 ± 0.45	9.22 ± 0.66	8.03 ± 0.24

Note: Values are shown as gold particles per area (N/μ^2) ± standard error of the mean. Statistical analysis revealed no significant differences between neuronal compartments.

2

1

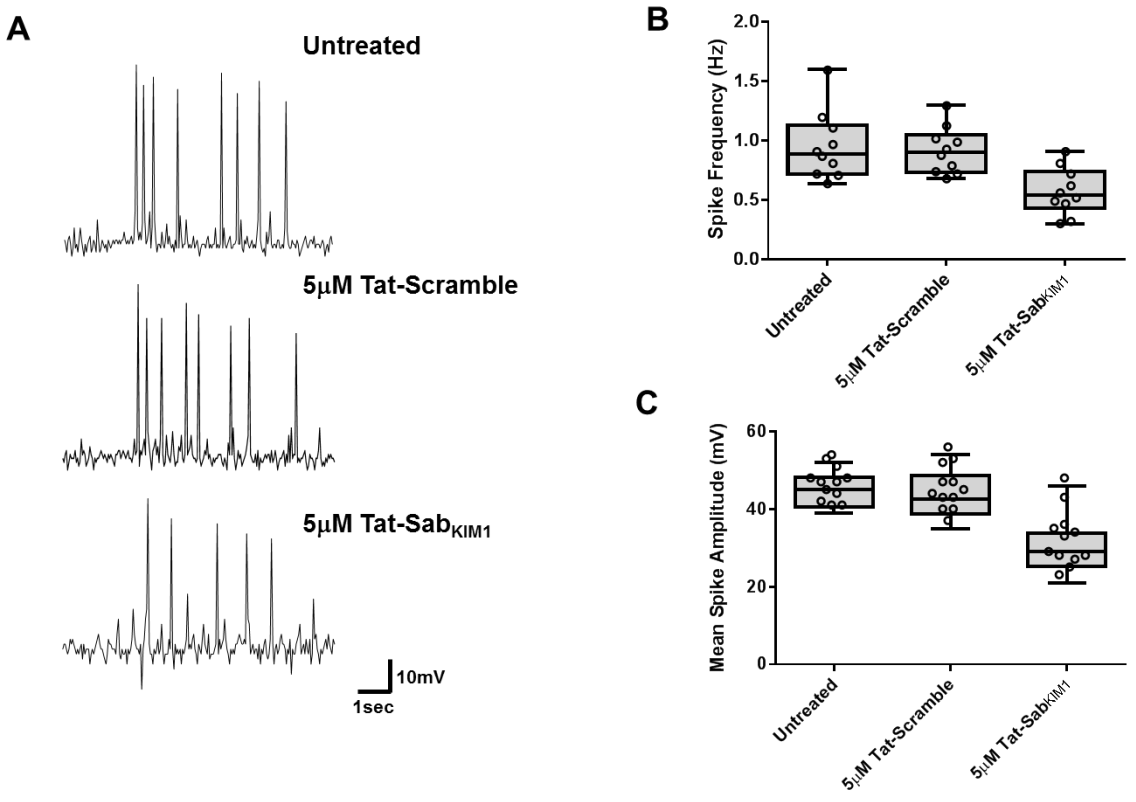
A
Untreated
5μM Tat-Scramble
5μM Tat-SabKIM1
10mV
1sec
B
Spike Frequency (Hz)
2.0
1.5
1.0
0.5
0.0
Untreated
5μM Tat-Scramble
5μM Tat-SabKIM1
C
Mean Spike Amplitude (mV)
60
40
20
0
Untreated
5μM Tat-Scramble
5μM Tat-SabKIM1

2